Fire Safety Engineering Research Group

16 July 2019

THE UNIVERSITY OF QUEENSLAND
AUSTRALIA
CREATE CHANGE

Protocols for the Material Library of Cladding Materials

Part II: Sample preparation and testing methodologies

Contents

1 Background

The “*Material Library for Cladding Materials*” project provides a wide set of results corresponding to materials and products used in cladding systems. The data provided is for a specific set of materials and products, therefore, other organisations might wish to apply the same principles for the testing of different materials or products. This document provides background information that enables a transparent disclosure of all procedures so that this data can be reproduced by others or for further testing to be conducted beyond the scope of the Material Library project.

The test methods and apparatus described are those which were used on the Material Library project. Other chemical analytical techniques or experimental approaches can be used for the same objectives, nevertheless, the use of alternative methods is not part of the Material Library project and therefore will not be discussed here.

The tests are conducted as much as possible in accordance with standardised methods, nevertheless, the nature of the materials will require specific deviations that will be discussed in this document.

Only the methods adopted are described in this document. For alternate and supplemental means of preparation or error and uncertainty estimation refer to the “*Protocols for the Material Library of Cladding Materials – Part III: Sensitivity studies*” [1] document.

The general preparation methods for all samples is briefly outlined. For each test apparatus, the preparation specific to that experiment is described in detail. The following testing methodologies are described in this document:

- Part A1 – Attenuated total reflectance Fourier transform infrared spectroscopy (ATR-FTIR) for material identification;
- Part A2 – Energy dispersive X-ray fluorescence (EDXRF) for elemental analysis and material quantification;
- Part B – Thermogravimetric analysis (TGA) for thermal decomposition;
- Part C – Bomb calorimeter for determination of gross heat of combustion;
- Part D – Mass loss calorimeter (MLC) for ignition properties;
- Part E – Cone calorimeter for evaluation of burning behaviour; and
- Part F – Lateral ignition and flame spread test (LIFT) for determination of flame spread properties.

The first three parts (A1, A2 and B) constitute the screening protocol while all seven parts (A1, A2, B, C, D, E and F) constitute the detailed testing protocol. The overall background to the project and guidelines for the use of the resulting data are described in more detail in “*Protocols for the Material Library of Cladding Materials – Part I: Framework*” [2].

2 General sample preparation

2.1 Sample collection

2.1.1 Screening protocol

A hole-saw was used to collect 40 mm diameter disc samples from relevant cladding products on buildings. This was performed by a contractor, and had both the building owner and the project fire engineers present during collection. Where larger samples were collected, for example, 100 × 100 mm square panels, then these were cut into a 40 mm circular disc. The resulting hole in the cladding from where the sample was taken had to be filled with a suitable material to protect the building. Samples were taken from all products part of the façade system, including aluminium composite panels (ACP), insulation (INS) and sarking (SRK) behind, and metallic sheets (DIS). Each of these was then considered as a single sample. This sample is unique and specific to the location from where it was extracted. The collection process is covered in more detail by guidance documents published by the Queensland Government [3].

The samples were labelled to include key information as follows:

- Code for the building or site;
- Building or block number, where relevant;
- Location of the sample on the building with reference to an annotated drawing, and which may include an indication of the height at which the sample was taken;
- Cladding layer from which the sample was taken, e.g. -A represents the outermost layer, -B represents the next inner layer, etc. up to -E, the innermost cladding layer;
- Each sample also separately contains a unique QR code which allows lookup of the full ID as needed.

A list of potential example IDs similar to those used on the project are given in Table 1. These labels should enable blind testing of the samples to eliminate potential bias, and thus should not contain any identifying information. Therefore the building code should not take the form of the building name.

Table 1 – A list of example IDs for cladding samples.

Example ID	Sample location description
BLDG-A-L01-A	Building A, location 01 at low height†, first layer (outermost)
BLDG-A-L01-B	Building A, location 01 at low height†, second layer
BLDG-A-L02-A	Building A, location 02 at high height†, first layer (outermost)
BLDG-A-L02-B	Building A, location 02 at high height†, second layer
BLDG-A-L02-C	Building A, location 03 at high height†, third layer (innermost)
BLDG-B-S01-A	Building B, location S01†, first layer (outermost)

†Note: Exact sample locations would be on an accompanying drawing available to engineers the building owner but not given to those who perform the testing.

Samples were stored in individual plastic pouches with a ziplock for adequate protection and then collated in batches corresponding to the site or building. Upon arrival to the testing laboratory, all samples were cleaned using 70% isopropyl alcohol wipes. All tools and surface areas were also cleaned with 70% isopropyl alcohol wipes between every sample preparation and test to avoid cross-contamination.

2.1.2 Detailed testing protocol

The detailed testing protocol involves larger-scale test methods and thus requires substantially more material for testing. The recommended quantity of material to adequately cover all the test methods is a 1×1 m panel. This also contains sufficient material to be able to run the screening protocol described above. The detailed testing protocol is typically run on samples which have already been screened and identified as of interest. Thus, detailed testing samples which are received are first rescreened to verify that the material matches the intended previously identified material. The process between the screening and detailed testing protocols is described in detail in the accompanying guidance document "*Protocols for the Material Library for Cladding Materials – Part 4: Use and interpretation*" [4].

2.2 Aluminium composite panels (ACP)

ACP samples provided will consist of the core and both metal skins intact. The metal skin is removed for all testing so that results are representative of the core of the ACP (Figure 1). The weight and thickness of the skin are taken in order to calculate the density and ascertain the composition of the metal quickly.

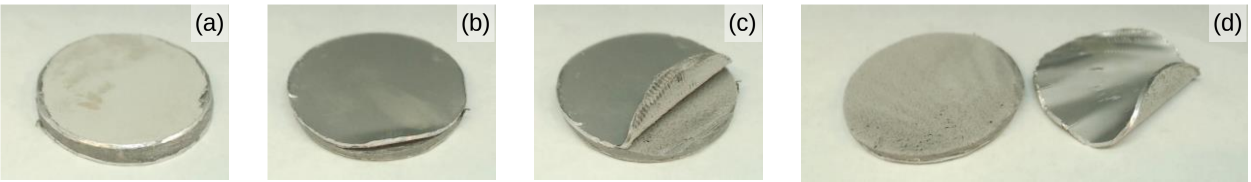

Figure 1 – Sample preparation process (a) sample as received from building (b) incision along the intersection of core and metal skin (c) beginning of peeling using pliers (d) metal skin completely removed.

The metal skin of ACPs will commonly have a thin polymer layer – such as a paint coating or a protective layer – on the surface. It is likely that each side will have a different coating, since they fulfil different functions. The protective coatings are generally 50-200 μm in thickness which is much smaller than the thickness of the aluminium plate (0.5 mm) or the core material (3–5 mm). Preliminary testing demonstrated that the surface coatings can be considered to have a negligible effect on the fire performance of the aluminium plates, and therefore they will not be considered as part of the information provided by the "*Material Library for Cladding Materials*" project.

2.3 Insulation materials (INS)

Insulation materials can be single materials or they can be part of a product with multiple components acting as a composite. The most common scenarios are those of an insulation material encapsulated (or partially encapsulated) by means of a metal sheet or an insulation material encapsulated or partially encapsulated by a very thin metal foil.

For the screening protocol, insulation which has a metal sheet as encapsulation (e.g. sandwich panels) will have this removed and tested as a different sample. The metal sheets will fall under the DIS category and will have their composition determined, as described in *Section 2.5 – Metallic sheets*. The core insulation product will undergo the standard screening protocol that consists of:

i. material identification
ii. chemical composition determination
iii. thermal decomposition assessment

For materials which contain a metal foil as encapsulation, then this is generally discarded and no testing of the foil is performed. Testing on the core insulation continues as normal and is presented in the database.

For detailed testing, the encapsulation is also removed. In some cases, a thin layer of adhesive is present bonding the metal foil or sheet to the bulk of the insulation. Compared to the bulk of the insulation, the adhesive makes up very little (<1%) of the overall mass and has a negligible contribution to the fire performance of the material.

2.4 Sarking materials (SRK)

Sarking materials are protective membranes which are typically inner layers of a cladding system. They are products that often contain multiple components and two different surfaces, one of which is normally reflective in the form of aluminium foil. Polymer surfaces commonly take two forms: either as a backing material to provide mechanical properties/protection, or as a protective coating applied to a carrier foil. In the case where they serve as a backing membrane/protective coating then the polymer makes up a substantial part of the sample.

1. Those which form a major component are put through all parts of the screening process. The polymer is peeled away from any aluminium backing, and tested by itself. This is done to remove contamination of the results by the aluminium, and ensure that positive identification can be made.
2. Polymers which are used as coatings are identified using ATR-FTIR but generally the amount of material is insufficient to test them using the TGA or EDXRF. As a result, the polymer is identified but not quantified.

2.5 Metallic sheets (DIS)

The nature of the framework is that all cladding materials in a system are tested. As a result, metallic sheets are included in the library under the label DIS. Any reference to metallic discs refers to these metal sheets. The metallic sheets might have polymer coatings which have very limited thickness and can only be tested using ATR-FTIR. The impact of these coatings is assumed to be of secondary importance compared to other materials in buildings, and thus fall outside the scope of the project at present. This was previously assessed using preliminary testing of ACP samples. Therefore, the coating is removed via sanding with 120-grade sandpaper and the composition of the metal sheet is determined and presented.

3 Attenuated total reflectance Fourier transform infrared (ATR-FTIR)

FTIR with an ATR accessory is an analytical technique to identify chemical components in a material by measuring their infrared spectrum (ASTM E1252 [5]). The technique operates by directing an infrared (IR) beam towards a crystal with a high refractive index, such as diamond or germanium. This creates an evanescent wave which will interact with a sample placed in direct contact with the crystal. A specific molecular vibration mode will absorb a characteristic wavelength, and this attenuation at that specific wavelength or spectral region is then measured by the detector. Each material has a specific fingerprint in the form of its absorbance spectrum which in turn allows qualitative identification of specific compounds.

This equipment allows testing of samples with only minimal preparation so that a high throughput can be attained. This reduces the time taken to test samples, reduces the resources needed, and reduces complexity in the process which enhances repeatability and reproducibility of results. In addition, the potential for contamination due to extensive sample preparation is reduced.

For samples with simple composition, e.g. pure synthetic polymers, the process of identifying the compounds is straightforward. For samples with multiple components then the process becomes more difficult, as the components may absorb at the same characteristic wavelength regions and consequently cannot easily be separated. For these cases, cross-referencing with the other techniques in the screening protocols is required to ensure confidence in identification and quantification.

Figure 2 – Thermo Fisher Scientific Nicolet iS50 FTIR spectrometer with Raman and diamond ATR accessory.

3.1 Sample preparation

Thin slices (10–15 mm length and 3 mm wide with the minimum possible thickness, in the region of 0.1–0.5 mm) were taken from the side of every sample to give the best depiction of the composition throughout the depth. The tested side of this slice was then always towards the centre of the sample, away from the effect of any extraction tool used to obtain the sample from the building. Each individual component was tested in samples where there were clear heterogeneities, for example, samples with sealant attached or containing multiple polymers.

3.2 Equipment and methodology

A Thermo Fisher Scientific Nicolet iS50 Fourier Transform Infrared spectrometer (FTIR) with attenuated total reflection (ATR) accessory was used (Figure 2). The in-built ATR accessory uses a monolithic diamond ATR crystal and an enhanced Lanthanum α Alanine doped TriGlycine Sulphate (DLaTGS) detector. Specimens in the form of thin slices, as described above, were placed directly on the diamond crystal and pressure was applied using a screw dial to ensure adequate contact between the sample and the material. Tests were performed in the spectral range of 4000–400 cm^{-1} (mid-field IR) with a spectral resolution of 4.0 cm^{-1}. For each sample, 32 scans were averaged and testing was repeated in three different locations. These three results were then checked and averaged again to give the final spectrum as presented in the library. Between each experiment, the crystal was cleaned using a 70% isopropyl alcohol wipe and dried, and the tools used were cleaned in the same manner in order to prevent cross-contamination. Additionally, a baseline scan of the background was performed before every sample and an advanced ATR correction was performed. This method corrects for spectra shifts and intensity changes in ATR and ensures the spectrum obtained is comparable to spectra obtained in transmission mode. The detail of the correction method is described by the manufacturer [6].

4 Energy dispersive X-ray fluorescence (EDXRF)

Energy dispersive X-ray fluorescence (EDXRF), or simply X-ray fluorescence (XRF), is an analytical technique (ASTM D6247 [7]) to quantify the elemental composition of materials. When used in tandem with FTIR or another technique capable of compound identification, then it can be used to quantify the specific compounds identified through an iterative process.

EDXRF uses high-energy X-ray radiation to deliver energy to atoms at sufficient intensity to cause electrons to be ejected. The electrons reach an excited state and emit fluorescent X-ray photons at specific wavelengths which can be measured by a detector. A continuous spectrum is obtained which is compared against the known wavelengths for specific elements to enable the qualitative identification. Additionally, the emission of each electron for a specific element has an associated intensity which can be measured over the duration of a test. The use of this intensity then enables the quantification of the elements in a material. Finally, oxygen (O) is one of the quantities that cannot be directly measured using XRF. Therefore, if compounds are identified using ATR-FTIR then they are added into the calculation method for XRF, and the quantification of compounds can be performed. From this, the chemical composition of a material is known and is presented in the Material Library.

The emission of photons from an atom may cause secondary interactions in other atoms. It is necessary to account for this, and for the shielding effect which may be caused by heavier elements. Both of these effects are compensated through the use of a standard-less method provided by the manufacturer, which is discussed in more detail below in *Section 4.2 – Quantitative XRF analysis*.

4.1 Qualitative XRF analysis

The elemental composition is determined from the collected XRF spectrum via a peak search and peak match algorithm. The peak search uses a mathematical method to find all peaks present in the spectrum, and the match algorithm matches the identified peaks with the known major fluorescent lines from a database. Due to the discrete nature of the major lines, qualitative XRF analysis is very robust and allows the accurate identification of all elements heavier than Neon (Ne). The S2 Puma EDXRF analyser used in this project was equipped with a light element detector (HighSense LE) which has a high sensitivity to light elements and allows detection of elements with atomic numbers equal to or larger than Carbon (C).

4.2 Quantitative XRF analysis

The aim of the quantitative XRF analysis is to determine the elemental concentrations of all elements present in the sample. This is done by correlating the net line intensities to the concentration. This process is complicated because the line intensities are not linearly proportional to the concentration. The intensity of an analytical line is influenced by the presence and concentration of other elements present in the sample. For standard-less analysis, *fundamental parameter matrix correction models* are used to account for all the possible interactions between elements based on a physical model of the X-ray interactions.

The fundamental parameter model, which forms the basis of the standard-less analysis process, captures all physical components that govern the primary fluorescence. In order to determine the concentrations with the fundamental parameters model, equipment specific parameters need to be known. For samples containing multiple compounds, the fundamental parameters model needs to be evaluated iteratively to ensure all measured intensities correspond to the model prediction.

The exact chemical composition for all compounds present in the sample is required in the fundamental parameters model, and thus essential to be able to provide accurate concentration results. This is particularly critical for oxygen-containing compounds because the oxygen atom has a strong shielding effect but it cannot be quantified directly from the XRF analysis. Identifying the exact compound from qualitative XRF analysis can be challenging as it is not always possible to identify the compound based on the elemental composition. This is particularly true for samples which contain multiple minerals with varying degrees of purity.

4.3 Sample preparation

Entries in the Material Library were cryogenically grinded into a homogeneous powder and then pressed into a thin film pellet. This is the method recommended by the manufacturer to give the most reliable results. The use of other preparation methods – for example, milling or sanding – are covered in the guidance document "*Protocols for the Material Library of Cladding Materials – Part III: Sensitivity studies*" [1].

4.3.1 Aluminium composite panels – Cryomilling

Cryogenic milling is a technique of breaking a material down into a powder using very low temperatures. In this project, samples were chilled below −100 °C using liquid nitrogen. This method avoids heat-induced degradation of the samples and allows thermoplastics – which are very tough at room temperature – to be ground into a homogeneous distribution of equally sized particles. This is particularly important for many ACPs on the project which contain thermoplastics. Other faster and cheaper techniques can be used but none can guarantee that heat-induced degradation is avoided.

4.3.2 Aluminium composite panels – Hot pressing

Hot pressing was used to form thin fused film samples with a thickness of 1 mm. The information depth of the XRF is very small (<15 µm), and so the thin film is sufficient that all the relevant elements can be detected. Hot pressing was performed using a Carver 30 t hot press where the sample was placed between two heated metal plates and compressed until the desired film thickness was achieved. The following conditions were found to be optimal for the majority of samples:

1. Cover platens with Teflon release film;
2. Place the cryomilled powder sample in the centre of platen;
3. Heat the platens to 170 °C and apply only enough pressure to maintain contact for 15 min. This temperature was selected primarily to avoid the degradation of common inert fillers or fire retardants, such as alumina trihydrate;
4. Apply pressure until desired film thickness is obtained;
5. Cool the plates to 40 °C and whilst keeping a constant pressure; and
6. Remove samples from platens.

4.3.3 Metallic sheets – sanding

Metallic discs which had a flat surface and sufficient thickness were sanded using 120-grade paper in a belt sanding machine. Additional polishing/sanding was performed as necessary by hand with 180-grade sandpaper. The sandpaper was then replaced between preparation of samples to prevent contamination. For discs which were thin (<0.5 mm) or deformed, then they could not be used in the sanding machine and were instead prepared by only by hand.

4.4 Equipment and methodology

All testing was performed using a Bruker-AXS S2 Puma XRF spectrometer with carousel and light element detector. Circular samples with a maximum diameter of 40 mm were placed in a holder inside a lead chamber which had the environment purged using a pump to attain a high vacuum. An X-ray tube with Ag anode and Be window with a maximum power of 50 W was used in this project to generate the radiation. Samples were analysed using 20 kV with no filter, 40 kV with a 500 µm aluminium filter, and 50 kV with a 250 µm copper filter in order to give a range of excitation conditions and accurately determine the elements. The resulting continuous spectrum was measured from 0 to 50 kV with the associated intensity at each wavelength.

The high vacuum was attained in the chamber by pumping out the atmosphere and maintaining this state for the duration of the test. A high vacuum was defined as a pressure below 6 mbar. The pressure was measured throughout to ensure that the vacuum was maintained, and the test was automatically terminated if this state was lost.

A calibration procedure and check for drift was performed every day. The procedure involved the quantitative standard-less analysis of a set calibration disc containing Na_2O, SiO, K_2O, CaO, MnO, As_2O_3, MoO_3 and Sb_2O_3. This disc was manufactured by FluXana (Bedburg-Hau, Germany) as FLX-K04 / BAXS-S2.

XRF analysis provides identification and quantification of inorganic elements and, when paired with other techniques, quantification of compounds in a material. Once the inorganic fraction of the material has been quantified, to calculate the organic component, e.g. the polymer portion of an ACP, then the organic content is assumed to be the remaining fraction of the mass of a sample. The XRF can miss some inorganic content, therefore, this calculation always provides a conservative measure of the polymer. Therefore, in the Material Library, the mass fractions are often presented using the mathematical less than symbol, <, to signify that this is the maximum expected quantity of polymer.

5 Thermogravimetric analysis (TGA)

Thermogravimetric analysis (ASTM E1131 [8]) is used to analyse the thermal decomposition of materials as a function of temperature. Reactions where mass loss occurs, such as pyrolysis and oxidation, can be identified using this technique. TGA is included in this testing protocol to enhance the robustness of the framework. The other material identification and quantification techniques are in theory sufficient but the addition of an extra technique to verify the results ensures that potential error is reduced.

Samples are placed within a small-scale furnace which heats up slowly at a user-defined temperature rate. A highly accurate load cell then measures the mass loss as a function of the temperature measured in the sample. The use of oxidising and inert atmospheres then provides insights into the identification and behaviour of materials. For example, some polymers (e.g. phenolic resins or polycarbonate) will yield char in an inert atmosphere which will oxidise when tested in air. The temperature at which this occurs can give some understanding into the behaviour of a material at elevated temperatures, although the mechanisms are more complicated and do not allow direct translation into fire performance.

Figure 3 – Netzsch Jupiter STA449 F3 used for analysing the thermal degradation of all samples.

5.1 Sample preparation

TGA samples were taken from the side of a given specimen so that data was averaged across the depth, as was the case for ATR-FTIR. The outer most layer was first removed in order to eliminate the effect of the sampling tool. Specimens took the form of small flakes (0.5–3 mm in length) to minimise the thermal gradients through the sample. These were lightly pressed into the bottom of the crucible to ensure good thermal contact with the thermocouple on the load cell. The sample mass is defined in the following section.

5.2 Equipment and methodology

All experiments were performed using a Netzsch Jupiter STA449 F3 (see Figure 3) with the following conditions:

- Constant heating rate of 20 °C min^{-1} from 50 to 800 °C. A ten-minute isothermal heating regime in air was added at the end of each test to prevent crucibles from becoming stuck to the load cell;
- One test in air atmosphere and one test in nitrogen atmosphere, for a total of two tests per sample;
- A flow rate of 150 ml min^{-1} for the gas, with an additional 20 ml min^{-1} nitrogen purge flow in all cases;
- Alumina crucibles (Al_2O_3) with a volume of 85 µl, a diameter of 6.8 mm, and without lids were used;
- Sample mass in general cases was 10.0 mg with a maximum deviation of 2.5 mg. Nonetheless, for some samples, this was not possible for the crucible volume, and so the target mass was reduced. A summary of typical mass changes is given below, and the averages are given in Table 2.
  - Wool-based insulations (e.g. INS03, INS08, INS09) had their mass reduced to 5.0 mg;
  - Sarking materials (SRK group) had their mass reduced to 5.0 mg;
  - Foam-based insulations (e.g. INS01, INS02, INS04, INS05, INS06, INS10) had their mass reduced to 2.5 mg; and
  - Materials which contained only a thin layer of adhesive (e.g. ACP06, ACP10, ACP28) had their mass reduced to 1.0 mg.
- The actual mass of the sample does not alter the results of the TGA, and where a range of mass is recommended, this is only to conduct the test within the optimal operation range of the load cell. Thus, this information is only presented for completeness.
- All results presented in the library use only the TG (thermogravimetry) function and do not use STA (simultaneous thermogravimetric analysis).

Table 2 – Summary of the actual average mass and standard deviation of TGA samples.

Material type	**Mass [mg]**
General samples	10.3±0.4
Wool-based insulation	5.2±0.3
Sarking	
Foam-based insulation	2.5±0.2
Adhesive/resins	1.0±0.1

6 Bomb calorimeter

The oxygen bomb calorimeter is used to determine the gross heat of combustion of fuels. A small quantity of sample (1.1 g maximum) is placed inside a sealed chamber filled with pure oxygen. The surrounding volume is filled with water and the temperature is measured accurately using a highly precise thermistor. A fuse wire is used to ignite the sample, and the temperature increase in the surrounding water allows the calculation of the total energy released. With the mass of the sample, this then enables calculation of the gross heat of combustion.

The methodology used was conducted according to the ISO 1716 standard [9] and guidance from the manufacturer. Additional details of the sample preparation and number of trials is given below, and the apparatus is shown in Figure 4.

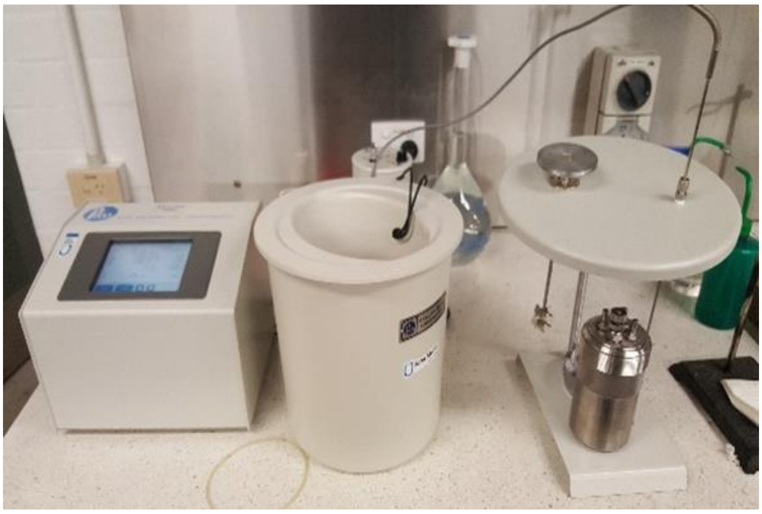

Figure 4 – Bomb calorimeter using a Parr Instruments (Moline, USA) Calorimetric Thermometer Model 6772.

6.1 Sample preparation

As per the recommendation in the standard, the samples were broken into several large pieces. This was in order to increase the surface area and give a more accurate and consistent value of heat of combustion. Some materials will not readily ignite. For these, a material ("the pill") with a known heat of combustion – benzoic acid – was used to ensure that ignition was achieved and that sufficient energy was released. The contribution of the pill was then removed and the gross heat of combustion of the actual sample was calculated. A list of these samples is given below in Table 3. In each case, unsuccessful ignition was first attempted without the pill.

Table 3 – Summary of samples which required the use of a material with known heat of combustion.

UQ ID	Sample description	Notes
ACP01	Aluminium composite panel with predominantly inorganic content.	Sample contains only 10% organic content and so the gross heat of combustion of the material is very low and requires the benzoic pill to achieve ignition.
ACP06	Aluminium composite panel with a core consisting of an aluminium egg-box profile core bonded with adhesive.	Only limited quantities of adhesive could be collected and so the benzoic pill was used to achieve ignition.
ACP10	Aluminium composite panel with a core consisting of a honeycomb-structure aluminium foil bonded with an adhesive.	Only limited quantities of adhesive could be collected and so the benzoic pill was used to achieve ignition.

6.2 Equipment and methodology

The equipment used was the Bomb calorimeter manufactured by Parr Instruments (Moline, USA) Calorimetric Thermometer Model 6772. Each material in the library had three bomb calorimeter tests performed. The following measurements are required in order to calculate the gross heat of combustion:

- Mass of the sample (g)
- Initial length of the fuse wire (cm)
- Final length of the fuse wire (cm)
- Calibration constant of the bomb (J °C^{-1})

A standardisation run using a fuel of known composition determined the energy equivalent of the calorimeter to be 10,315.91 J K^{-1}. Results were also corrected for the contribution of the fuse wire by applying a correction factor of 9.632 J per cm of fuse wire consumed during the test. The gross heat of combustion is calculated according to Eq. 1:

$$\Delta H_c = \frac{W\,\Delta T - \Delta L_{fuse}\,e_1}{m} \qquad \text{Eq. 1}$$

where W is the energy equivalent of the calorimeter, ΔT is the temperature increase, e_1 is the heat of combustion of the fuse wire per cm consumed, and m is the mass of the sample. The heat of combustion is then presented for: each individual trial, an average of all the trials, and the standard deviation of all the trials.

7 Mass loss calorimeter (MLC)

A standalone conical heater was used to measure the ignitability of samples. This is the same as the cone calorimeter (ISO 5660 [10]) but no gas analysis was performed. Furthermore, a key difference was that experiments were terminated as soon as the ignition data was recorded to allow a higher throughput of tests to be performed.

The following properties are presented in the library:

- Critical heat flux (kW m^{-2})
- Ignition temperature (°C)
- Total heat transfer coefficient of losses (W m^{-2} K^{-1}) at the ignition temperature
- Apparent thermal inertia (kW^2 m^{-4} K^{-2} s)

7.1 Sample preparation

The sample preparation was as per Annex H in ISO 5660, and is described comprehensively in the cone calorimeter, in *Section 8.1– Sample preparation*. The following modification to Annex H was added:

- All tests that required the fine mesh (those samples listed in the cone calorimeter section) had the retainer frame in position to be able to keep the mesh in place.

This modification was implemented due to excessive expansion of samples, particularly in ACPs.

7.2 Equipment and methodology

All testing was performed using a conical heater provided by Fire Testing Technology (East Grinstead, UK) according ISO 5660 but without the gas analysis or load cell.

The data that is recorded is (a) whether ignition occurs or not and, if so, (b) the time to ignition. Experiments were performed until there were data points with and without ignition within a range of approximately 1 kW m^{-2}.

The criteria for ignition were based on Annex H of ISO 5660 and were as follows:

- Ignition was recorded when there was sustained flaming for more than 10 s;
- If there was flash flaming, then the spark ignitor was not removed until sustained flaming was achieved;
- Ignition must occur within 15 min (900 s) to be considered valid; and
- The critical heat flux (kW m^{-2}) was determined as the average between the highest heat flux at which no ignition occurred and the lowest heat flux at which ignition did occur.

7.3 Determination of properties

The piloted ignition temperature, T_{ig}, is assumed to correspond to the pyrolysis temperature, T_P, since the induction time and the mixing time can generally be neglected under the specific conditions of this testing method. The critical external heat flux for piloted ignition, $\dot{q}''_{cr}$, obtained experimentally can then be used to determine the piloted ignition temperature.

The particular formulation considered for this work is the one presented by Long *et al.* [11]. The time to achieve the ignition temperature at the surface of the solid material can be obtained according to Eq. 2:

$$\frac{(T_{ig} - T_\infty)}{T_c} = \left[1 - \exp\left(\frac{t_{ig}}{t_c}\right) \cdot \operatorname{erfc}\left(\left(\frac{t_{ig}}{t_c}\right)^{1/2}\right)\right] \qquad \text{Eq. 2}$$

where T_{ig} and t_{ig} are the temperature and time of ignition respectively, T_∞ is the ambient temperature, erfc is the complementary Gaussian error function, T_c is the characteristic surface temperature defined as Eq. 3 and t_c is the characteristic time defined as Eq. 4:

$$T_c = \frac{a\,\dot{q}''_e}{h_T} \qquad \text{Eq. 3}$$

$$t_c = \frac{k\rho c}{(h_T)^2} \qquad \text{Eq. 4}$$

where a is the absorptivity of the exposed surface, $\dot{q}''_e$ is the external heat flux, h_T is the global heat transfer coefficient of losses and $k\rho c$ is the thermal inertia. The global heat transfer coefficient of losses, at the time that the surface achieves the ignition temperature, can be defined as:

$$h_T = h_{conv} + h_r = h_{conv} + \varepsilon\,\sigma\,\left(T_{ig}^2 + T_\infty^2\right)\left(T_{ig} + T_\infty\right) \qquad \text{Eq. 5}$$

where h_{conv} is the convective heat transfer coefficient, ε is the emissivity of the surface, σ is the Stefan–Boltzmann constant and T_∞ is the ambient temperature. The definition of the convective heat transfer coefficient is based on the estimation of the Nusselt number for the free convection of a horizontal hot plate [12], as noted in Eq. 6:

$$\overline{Nu}_L = 0.54\,Ra_L^{1/4} = \frac{h_{conv}\,L_c}{k_{air}} \qquad \text{Eq. 6}$$

where Ra_L is the Rayleigh number, k_{air} is the conductivity of the air, and L_c is the characteristic length.

The ignition temperature can be calculated assuming that the steady-state is achieved for the heat balance at the surface. For this case, the net heat flux through the surface of the material can be assumed to be null, i.e.:

$$\dot{q}''_{net} = -k\left.\frac{\partial T}{\partial x}\right|_{x=0} \approx 0 \qquad \text{Eq. 7}$$

where k is the conductivity of the material and $\left.\frac{\partial T}{\partial x}\right|_{x=0}$ is the thermal gradient at the surface. The potential inaccuracy of this approach due to non-negligible values of the net heat flux through the solid surface during the steady-state has been previously indicated by Mowrer [13]. The heat balance at the surface is nonetheless assumed to be expressed as:

$$a\,\dot{q}''_{cr} - h_T\left(T_{ig} - T_\infty\right) = \dot{q}''_{net} \approx 0 \qquad \text{Eq. 8}$$

Therefore, the expression to calculate the ignition temperature can be written as follows:

$$T_{ig} = T_\infty + \frac{a\,\dot{q}''_{cr}}{h_T} \qquad \text{Eq. 9}$$

It should be noted that since the total heat transfer coefficient depends on the surface temperature, the ignition temperature and the total heat transfer of losses are calculated by solving iteratively the system of non-linear equations consisting of Eq. 5 and Eq. 9.

For heat fluxes significantly larger than the critical value, a Taylor series expansion is performed around $t_{ig}/t_c \rightarrow 0$ on Eq. 2, leading to the following equation:

$$\frac{1}{\sqrt{t_{ig}}} = \frac{2}{\sqrt{\pi}} \frac{a}{\sqrt{k\rho c}} \frac{\dot{q}_e''}{(T_{ig} - T_{amb})} \qquad \text{Eq. 10}$$

Where 1/√t_{ig} is plotted across a series of series of heat fluxes, $\dot{q}_e''$, to be able to obtain the slope and calculate the apparent thermal inertia, as presented in the library. It is quite common to assume that the absorptivity equals to unity ($a \approx 1$) nevertheless, this assumption is not necessary and makes no difference to the approach given that the apparent thermal inertia can or cannot include an absorptivity term. For simplicity, in the Material Library the absorptivity will be approximated to unity and the apparent thermal inertia only defined by the term $k\rho c$.

8 Cone calorimeter

The cone calorimeter (ISO 5660 [10]) is a standardised bench-scale apparatus which is commonly used to obtain key flammability data of materials. A conical heater is positioned above a specimen designed to radiate a user-defined heat flux to the surface. As the surface heats up, the sample begins to decompose and generate pyrolysis gases. Once fuel production has allowed a mixture that is within the flammability limits at the location of the spark ignitor, the mixture will ignite and flaming combustion will be initiated. The resulting heat release rate, mass loss rate, time to ignition and gas generation can all then be measured. The experiments are performed over a range of heat fluxes to gain better understanding of the burning behaviour of the material. An illustration of an experiment after ignition is shown in Figure 5.

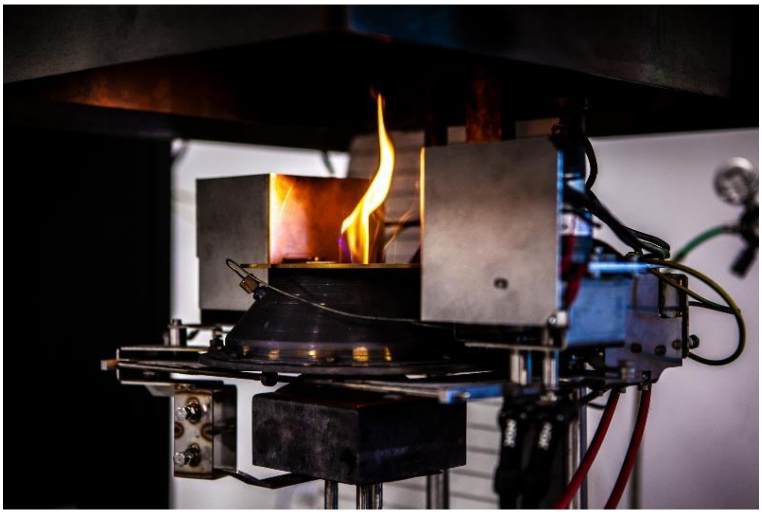

Figure 5 – Cone calorimeter (Fire Testing Technology, UK) during operation.

8.1 Sample preparation

Any protective layer was removed from the sample, as per the usual preparation described in *Section 2 – General sample preparation*. Unless otherwise noted, the methodology follows that of the standard ISO 5660 [10]. A summary of the preparation specific to the cone calorimeter experiments testing is given below:

- Samples were cut to 100 × 100 mm;
- The standard metal retainer frame was in place for all tests;
- A metallic grid was used in all tests unless otherwise noted. This was used to counteract (a) expansion upon heating, which is extremely common in fire retarded ACP samples, and (b) shrinkage/shrivelling of samples, which occurs in fabrics or textiles, and is mainly noted in SRK samples. The samples which did not use the grid are those which regress, for example, polystyrene foam (INS04) and polyester insulation (INS03).
- The rear surface was insulated with a minimum of one layer of 25.0 mm ceramic fibre wool insulation, and increasing to fill the thickness of the retainer frame for thin samples.
- All samples were wrapped in a single layer of foil to prevent the leakage of liquid material; and
- No thermocouples were placed in the sample.

8.2 Equipment and methodology

All testing was performed in a standardised ISO 5660 iCone Calorimeter (Fire Testing Technology, East Grinstead, UK).

The following steps were taken to perform the testing:

- Samples were exposed to three radiant heat fluxes of 35, 50 and 60 kW m^{-2}. In some cases 60 kW m^{-2} was replaced with 80 kW m^{-2} to give a better spread of results an ensure the performance was known at a higher heat flux;
- Samples were only tested in the horizontal orientation;
- The distance between the top of the specimen surface and the conical heater was set at 25 mm, and the spark ignitor was at positioned halfway between;
- The fan speed in the duct was set to the standard 24 l s^{-1};
- Gas analyser calibrations were performed once or twice a day as needed; and
- Heat flux calibration using a Schmidt-Boelter gauge was performed before every distinct heat flux for each sample.

The metrics recorded and presented in the Material Library are as follows:

- Heat release rate (kW m^{-2}) as a function of time
- Mass (g) as a function of time
- Peak heat release rate (kW m^{-2})
- Total energy released (MJ m^{-2})
- Time to ignition (s)
- Mass residue at the end of the test (-)
- Effective heat of combustion (kJ g^{-1})

The effective heat of combustion ($\Delta h_{c,eff}$) is determined using the following expression, as per the ISO 5660 standard:

$$\Delta h_{c,eff} = \frac{Q_T}{m_i - m_f} \qquad \text{Eq. 11}$$

where Q_T is the total energy released throughout the experiment (MJ), m_i is the initial mass (g), and m_f is the mass at the end of the test (g). The denominator therefore represents the amount of mass lost. This expression then gives an effective heat of combustion which is based only on the mass lost and not on the total mass. As a result, direct comparison with the gross heat of combustion previously determined using the bomb calorimeter for composite materials will not yield equivalent results.

9 Lateral ignition and flame spread test (LIFT)

The lateral ignition and flame spread test (ISO 5658 [14]) is used to determine the material-dependent flame spread parameter, Φ, and the critical heat flux for flame spread, $\dot{q}_{0,s}''$. A lengthwise specimen (600 × 100 mm × thickness) is positioned in front of a radiant panel at a specific angle to provide a predefined heat flux distribution. For the Material Library, the dimensions of the sample (given above) are reduced from the standardised 800 × 150 mm because of limited amount of material available. This has been shown not to alter the results Long *et al* [11]. For these tests, this was also verified by comparisons with common materials (e.g. plywood) which show similar numbers to the literature [15]. The reduction is necessary because the samples are taken directly from buildings and therefore the quantity of available material is restricted. The extracted flame spread parameter is based on flame spread velocities as a function of the incident heat flux.

9.1 Sample preparation

A tool was fabricated to aid the removal of the encapsulation of ACPs due to the larger scale when compared with the other parts of testing. This was to enable consistent removal along the length of sample, as well as reducing the time and mechanical strain of sample preparation. Samples were wrapped in a single layer of aluminium foil around the sides and back, and had two layers of 12.5 mm thick calcium silicate board as backing, for a total backing thickness of 25.0 mm. A wire mesh was introduced on the surface only for SRK group samples where there was substantial surface shrinkage/shrivelling.

9.2 General methodology and analysis

For the purpose of these tests, a bespoke assembly that fulfils the requirements of the standardised test was developed. A gas infrared porous burner was used as the radiant panel. The desired heat flux distribution was set for each specific material and a calibration was performed using a water-cooled Schmidt-Boelter gauge. Two layers of calcium silicate backing board had holes drilled along their length with diameters equal to the gauge head and located at distances of 50, 120, 190, 262, 334, 407, 475 and 550 lengthwise. The heat flux at 0 and 600 mm was assumed to be equal to the nearest heat flux measurement, at 50 and 550 mm respectively. A single gauge was used in each position sequentially until the desired heat flux and distribution was obtained. Adjustments to this were attained by (i) moving the panel closer or further away, while the gas flow of the panel was always kept constant, and (ii) changing the angle of the panel and the sample to vary the heat flux distribution along the length. The average normalised calibration of every test is given below in Figure 6, where the error bar is the standard deviation and the error for a single test or calibration will be significantly lower.

The sample was covered at the start of the test to allow the radiant panel to heat up and reach the normal operating conditions at which the calibration was performed. The test was started when the cover was removed, and the sample was exposed to the radiant panel. This was then the preheating time as the sample reached thermal equilibrium with the panel and environment. There was no pilot in place during this time. The definition of thermal equilibrium and hence the time to introduce the pilot is detailed in the sections below. Once equilibrium was reached, the pilot was introduced for 0–5 s until there was ignition and the flame front could begin to spread. The position of the flame front along the length of the specimen was recorded as a function of time using video camera recordings. The calibration allowed the heat flux to be determined at a specific location, and thus the flame spread velocity could be obtained as a function of the imposed heat flux. This is presented in the library, as well as the minimum heat flux required for flame spread, $\dot{q}_{0,s}''$, which is the lowest heat flux where there was flame spread, and the minimum spread velocity, $v_{f,min}$, which is an approximation of the velocity close to extinction.

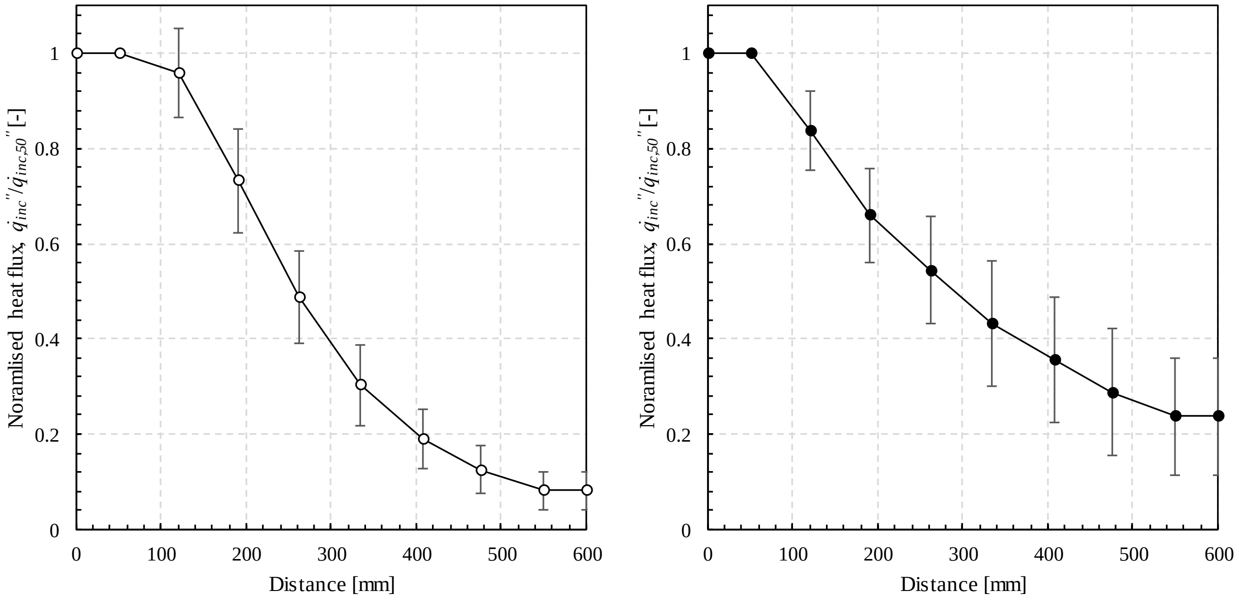

Figure 6 – Average distribution of all heat flux calibrations normalised to the incident heat flux measured at 50 mm for horizontal (left) and vertical (right) orientations. In all cases, the peak incident heat flux, $\dot{q}_{inc,50}''$, was set to be above the critical heat flux for piloted ignition. Error bars represent standard deviation.

The data is then transformed into a relationship of $1/\sqrt{V_f}$ as a function of the incident heat flux, $\dot{q}_{inc}''$ (or $\dot{q}_{ext}''$), in order to estimate the flame spread parameter, Φ. The transformation of the raw data results in an approximately linear relationship between $1/\sqrt{V_f}$ and $\dot{q}_{inc}''$, with the slope corresponding to $(k\rho c/\Phi h_T^2)^{1/2}$. The thermal inertia, *kpc*, critical heat flux ignition $\dot{q}_{cr}''$, and total heat transfer coefficient of loss (h_T) were determined previously using the mass loss calorimeter and cone calorimeter, which allows the flame spread parameter (in units kW^2 m^{-3}) to be calculated using the following equation, Eq. 12:

$$\Phi = \frac{k\rho c}{{h_T}^2} \times \frac{1}{{m_{fit}}^2} \qquad \text{Eq. 12}$$

The value of the flame spread parameter is then given for each test that was performed. To ensure repeatability, two tests were performed in each orientation (i.e. two tests in the horizontal orientation and two tests in the vertical orientation).

9.3 Methodology modifications

There are two main changes to the standardised methodology. Firstly, the testing was performed according to the research method originally proposed by Quintiere & Harkleroad [15]. This is reliant on the accurate determination of the critical heat flux and apparent thermal inertia, which were determined as part of the other testing specified previously in *Section 7 – Mass loss calorimeter (MLC)* and *Section 8 – Cone calorimeter* respectively. Secondly, additional testing was performed in the vertical orientation. The conditions used were the same as those in the horizontal lateral configuration but with the specimen rotated 90 degrees.

9.3.1 General

The two major components of the methodology are that the radiant heat flux imposed is reduced to a set level slightly above the critical heat flux, and that a preheating time is introduced to allow the sample to reach thermal equilibrium before a pilot is introduced.

The heat flux to be used in flame spread is suggested as 5 kW m^{-2} above the critical heat flux. For flame spread, the region of most interest is that below the critical heat flux for ignition, yet sufficiently above critical heat flux for flame spread and where the imposed heat flux as a function of the distance (Figure 6) is near linear. Near to either edge condition, the sample will be close to extinguishing or will be too close to near instantaneous flame spread. The area of most interest then is often relatively limited, particularly where the critical heat flux of ignition of a material is low compared to the standardised imposed incident heat flux of 50 kW m^{-2}. A typical value of critical heat flux of ignition for a specimen in the Material Library is less than 20 kW m^{-2}, and hence under standardised conditions more than half the data has no use since it is well above the critical heat flux for ignition. The purpose of this change therefore is to allow a higher resolution study of the key region of the sample.

Preheating is introduced to allow the surface to reach thermal equilibrium before ignition occurs. This ensures that external heating from the radiant panel is not occurring transiently while the flame is spreading and that it is instead in an approximate steady state. When there is not thermal equilibrium, the analysis requires the introduction of a correction factor, $F(t)$. This factor represents an adjustment to account for the error associated to the flame front arriving at a particular location before the temperature is in a steady state. The introduction of the preheating time thus allows simplification of the analysis by ensuring that $F(t) = 1$.

Thermal equilibrium was initially determined by an array of thermocouples (type K, 2.0 mm diameter) positioned along the length of the sample at a thickness close to the exposed surface. It was determined however that the thermal lag in the thermocouple resulted in a delayed reading, meaning that the preheating time was excessively long. The use of thermocouples with a smaller diameter improves the response time but can be more difficult to work with and have a higher failure rate. In subsequent tests, the thermocouples were removed and a preheating time was calculated based on the ignition times in the mass loss calorimeter and cone calorimeter testing. The added benefit of the removal of the thermocouples was that this prevented the thermal disturbance caused by the introduction of a foreign object in the sample.

It was found for pure, non-composite, non-flame retarded samples that the best value for imposed heat flux was 0–2 kW m^{-2} above the critical heat flux for ignition. For other samples, the imposed heat flux was maintained at 5 kW m^{-2} above the critical heat flux for ignition.

9.3.2 Vertical

Vertical LIFT experiments were introduced given their potential relevance for upward flame spread in cladding materials. At present, the LIFT apparatus and calculation method are not adjusted for upward flame spread and thus it should only be taken as a qualitative assessment.

Theoretically, vertical and lateral flame spread differs in that the former spreads co-current to the induced flow while the latter opposed to the induced flow, nevertheless, the analysis for the vertical orientation can be framed in a near identical form to that in the horizontal lateral spread configuration. A major difference is that the role of convective flow is more important in vertical spread.

In the vertical alignment, convective heating of the far end of the sample (i.e. the top) means that the heat flux can never be reduced to 0.0 kW m^{-2}. This effect can be seen in the representative calibrations shown in Figure 6, where the normalised heat flux $\dot{q}_{inc}''/\dot{q}_{inc,50}''$ was 0.24±0.12 (dimensionless) in vertical but could be reduced down to 0.08±0.04 in the horizontal configuration. The fact that there is no adequate heat flux distribution is not a serious complication, nevertheless, it makes it difficult to obtain a minimum heat flux for spread.

Lastly, the determination of the location of the flame front is significantly more difficult. For lateral spread, the flame tip exceeds the top of the sample and there is near constant flaming along the actual height of the sample. In many cases, particularly as the flame spread velocity reduces, the flame will “tilt” and the spread will progress faster along the top edge than the bottom edge. This can generally be alleviated by only tracking the progression along the mid-height of the sample, and then the process is relatively straightforward. In vertical, the intermittent flaming region and flame tip overlay with the virgin, unburnt material and the pyrolysis front. The presence of the flame also inhibits the ability to accurately observe the charring front for char-forming materials. Where possible, the flame front has been recorded as the most progressed location of the flame base i.e. where the flame is still attached to the sample. This is aided by the use of side camera but nonetheless proves difficult in many cases. Data for the vertical flame spread carries a significant error and should be used only as a reference value to assess relative performance. Quantitative use of this data for the purpose of estimating flame spread velocities requires detailed justification.

10 References

[1] M. Heitzmann, M.S. McLaggan, J.P. Hidalgo, A.F. Osorio, C. Maluk, D. Lange, J. Carrascal, J.L. Torero, (2019). P*rotocols for the Material Library of Cladding Materials – Part III: Sensitivity studies*. Fire Safety Engineering Research Group, UQMLCM2019-03. School of Civil Engineering, The University of Queensland. https://espace.library.uq.edu.au/view/UQ:1d87ca0.

[2] J.P. Hidalgo, M.S. McLaggan, A.F. Osorio, M. Heitzmann, C. Maluk, D. Lange, J. Carrascal, J.L. Torero, (2019). *Protocols for the Material Library of Cladding Materials – Part I: Framework*. Fire Safety Engineering Research Group, UQMLCM2019-01. School of Civil Engineering, The University of Queensland. https://espace.library.uq.edu.au/view/UQ:733236.

[3] Department of Housing and Public Works – Queensland Government, Guideline – For assessing buildings with combustion cladding, Version 2, (2019) 1–58. http://www.hpw.qld.gov.au/SiteCollectionDocuments/GuidelineAccessCombustibleBuildings.pdf.

[4] J.P. Hidalgo, M.S. McLaggan, A.F. Osorio, M. Heitzmann, C. Maluk, D. Lange, J. Carrascal, J.L. Torero, (2019). *Protocols for the Material Library of Cladding Materials – Part IV: Use and interpretation*. Fire Safety Engineering Research Group, UQMLCM2019-04. School of Civil Engineering, The University of Queensland. https://espace.library.uq.edu.au/view/UQ:0aec94c.

[5] ASTM International, ASTM E1252-98: Standard Practice for General Techniques for Obtaining Infrared Spectra for Qualitative Analysis, (2013) 13. doi:10.1520/E1252-98R13E01.

[6] S. Nunn, K. Nishikida, Thermo Fisher Scientific, Application Note: 50581 – Advanced ATR Correction Algorithm, (2008) 1–4. https://assets.thermofisher.com/TFS-Assets/CAD/Application-Notes/D10241~.pdf.

[7] ASTM International, ASTM D6247: Standard Test Method for Determination of Elemental Content of Polyolefins by Wavelength Dispersive X-ray Fluorescence Spectrometry, (2010). doi:10.1520/D6247-18.

[8] ASTM International, ASTM E1131-08: Standard Test Method for Compositional Analysis by Thermogravimetry, (2014). doi:10.1520/E1131-08R14.

[9] British Standards Institution, BS EN ISO 1716:2010 Reaction to fire tests for products — Determination of the gross heat of combustion (calorific value), Brussels, 2010.

[10] British Standards Institution, BS ISO 5660-1:2015. Reaction-to-fire tests — Heat release, smoke production and mass loss rate. Part 1: Heat release rate (cone calorimeter method) and smoke production rate (dynamic measurement), Brussels, 2015.

[11] R. Long, J.L. Torero, J. Quintiere, A.C. Fernandez-Pello, Scale And Transport Considerations On Piloted Ignition Of PMMA, Fire Saf. Sci. 6 (2000) 567–578. doi:10.3801/IAFSS.FSS.6-567.

[12] T.L. Bergman, A.S. Lavine, F.P. Incropera, D.P. DeWitt, Fundamentals of Heat and Mass Transfer, 7th ed., John Wiley & Sons, New York, 2011.

[13] F.W. Mowrer, An analysis of effective thermal properties of thermally thick materials, Fire Saf. J. 40 (2005) 395–410. doi:10.1016/j.firesaf.2005.03.001.

[14] British Standards Institution, BS ISO 5658-2:2006 Reaction to fire tests -- Spread of flame -- Part 2: Lateral spread on building and transport products in vertical configuration, 2006.

[15] J.G. Quintiere, M.T. Harkleroad, New Concepts for Measuring Flame Spread Properties, in: T.Z. Harmathy (Ed.), Fire Saf. Sci. Eng. ASTM STP 882, Philadelphia, PA, 1985: pp. 239–267. doi:10.1520/STP35300S.

11 Acknowledgements

This Material Library of Cladding Materials project was funded by the Department of Housing and Public Works (Queensland Government).

THE UNIVERSITY OF QUEENSLAND
AUSTRALIA
CREATE CHANGE

Contact details

Fire Safety Engineering Research Group

Dr Martyn S. McLaggan
Dr Juan P. Hidalgo
Dr Andres F. Osorio
Dr Michael Heitzmann
Dr Cristian Maluk
Dr David Lange
Mr Jeronimo Carrascal

Reviewed by Prof José L. Torero

E **fire-staff@civil.uq.edu.au**
W **www.civil.uq.edu.au/fire**

CRICOS Provider Number 00025B